Site-Selective Carbene-Induced C–H Functionalization Catalyzed by Dirhodium Tetrakis(triarylcyclopropanecarboxylate) Complexes

Kuangbiao Liao[1], Wenbin Liu[1], Zachary L. Niemeyer[2], Zhi Ren[1], John Bacsa[1], Djamaladdin G. Musaev[1,3*], Mathew S. Sigman[2*] and Huw M. L. Davies[1*]

[1]Department of Chemistry, Emory University, 1515 Dickey Drive, Atlanta, Georgia 30322.

[2]Department of Chemistry, University of Utah, 315 South 1400 East, Salt Lake City, Utah 84112

[3]Cherry L. Emerson Center for Scientific Computation, Emory University, 1521 Dickey Drive, Atlanta, Georgia, 30322.

ABSTRACT: Three types of dirhodium tetrakis(triarylcyclopropanecarboxylate) were generated and shown to adopt disparate high symmetry structures. These catalysts were evaluated in the intermolecular C–H functionalization of an array of terminally substituted *n*-alkanes and displayed various site selectivity as a function of catalyst and substrate structure, which could be correlated through quantitative relationships. Keywords: Site Selectivity, Non-Activated C–H bond, Enantioselective C–H Functionalization, Donor/Acceptor Carbene, Dirhodium Tetracarboxylate, Predictive Modelling

C–H Functionalization has inspired the imagination of organic chemists because it offers a modern strategic approach for the construction of complex molecules.[1] A major challenge is controlling site selectivity in molecules with multiple C–H bonds. Considerable progress has been made in the last several years by exploting the innate substrate reactivity[2] or by using directing groups to chelate with a metal catalyst to position it adjacent to the C–H bond to be functionalized.[3] Such approaches, however, do have natural limitations about what site in a molecule can be functionalized. A more versatile but challenging approach would be one in which the catalyst itself controls the site selectivity between similar C–H bonds and even overrides the inherent reactivity of a substrate.[4] In an ideal situation, one would have a collection of catalysts with different characteristics and then using predictive algorithms, select the best catalyst for the desired site selectivity.[5]

For some time, we have been exploring the dirhodium tetracarboxylate-catalyzed C–H functionalization reactions of donor/acceptor rhodium carbenes derived from aryldiazoacetates.[6] This system has become popular because it undergoes a wide variety of selective carbene reactions including intermolecular C–H functionalization of a range of substrates with high levels of site selectivity, diastereoselectivity, and enantioselectivity. Essentially all of the earlier work was conducted with Rh_2(DOSP)$_4$ (Figure 1) as the chiral catalyst, and even though it has broad utility, if a particular substrate gave a mixture of products, little could be done to improve the reaction outcome. Recently, we reported a new class of bulky, modular chiral ligands, 1,2,2-triarylcyclopropanecarboxylates (TPCP),[7] and demonstrated that their dirhodium complexes are capable of site selective reactions at activated primary C–H bonds, such as benzylic, allylic and sites alpha to oxygen, with a very different reactivity profile to that of Rh_2(DOSP)$_4$. Further refinement of these catalyst structures led to the development of the D_2-symmetric catalyst, Rh_2[*S*-3,5-di(*p*-^{t}BuC_6H_4)TPCP]$_4$,[8] capable of selective functionalization at the C2 position of *n*-alkanes or terminally-substituted *n*-alkanes (Scheme 1). Herein, we disclose the structural elements of two other members of the TPCP dirhodium family, Rh_2(*p*-PhTPCP)$_4$ and Rh_2(*o*-ClTPCP)$_4$. In addition, we compare the C–H functionalization site selectivity of the three types of catalysts and develop a quantitative model of the electronic effects of substrates for site-selectvity with the different catalysts. These studies identified three distinctive orientations for TPCP catalysts that adopt very different shapes, and demonstrate the utility of the quantitative model for the rapid assessment of new dirhodium catalysts.

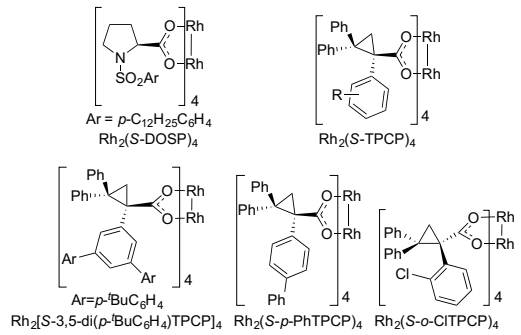

Figure 1. Chiral Dirhodium Catalysts

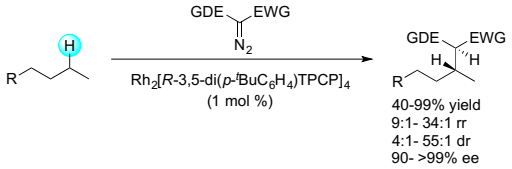

Scheme 1. Selective functionalization of 2° C–H bonds

A critical component of our design of chiral dirhodium-catalysts is the use of four identical carboxylate ligands, containing a structural feature within the ligand that is too sterically demanding to align in the periphery of the catalyst.[8,9] Thus, the large component must align on the α face or the β face of the catalyst, leading to four possible structural permutations, each having a different symmetry (Figure 2). In Davies' initial study on $Rh_2(DOSP)_4$ that introduced these design elements,[9a] they proposed that the catalyst could in principle adopt four orientations α,β,α,β (D_2 symmetric), α,α,α,α (C_4 symmetric), α,α,β,β (C_2 symmetric), and α,α,α,β (C_1 symmetric) (α represents the top face and β represents the bottom face of the catalyst). Further studies by Fox and Charette have shown that certain dirhodium catalysts adopting an α,α,α,α orientation may not be perfectly aligned and thus behave as if they are pseudo C_2 symmetric rather than C_4 symmetric.[10]

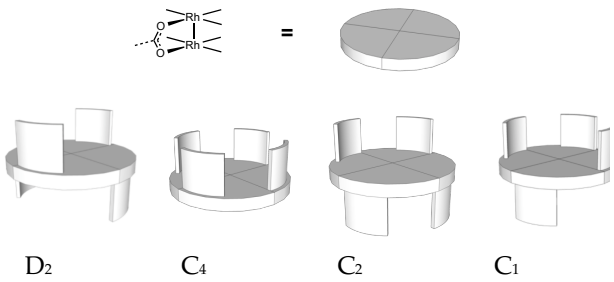

Figure 2. High symmetry orientations of dirhodium catalysts

The TPCP catalysts have a more sophisticated design element because both the C1 aryl and the *cis*-C2 (*cis* to carboxylate group) aryl groups are forced to align away from the periphery of the complex. In the case of Rh_2[*S*-3,5-di(*p*-^{t}BuC_6H_4)TPCP]$_4$, the C1 aryl group is so sterically demanding that if the C1 aryl of the first ligand is on the α face, then the C1 aryl of the adjacent ligand must be on the β face (Figure 3a).[8] The catalyst adopts an α,β,α,β orientation in the crystalline form, generating a structure that is D_2 symmetric. Corroboration that this is the preferred conformation was obtained through ONIOM studies of the slightly simpler derivative, Rh_2(*S*-3,5-diPhTPCP)$_4$, which revealed that the α,β,α,β form is 5.0 kcal/mol more stable than the α,α,α,α form.[8]

Encouraged by the remarkable site selectivity exhibited by Rh_2[*S*-3,5-di(*p*-^{t}BuC_6H_4)TPCP]$_4$, we continued to explore other members of the TPCP family of catalysts. Surprisingly, we found that depending on the aryl substitution, the complexes adopt different orientations. During the previous catalyst optimization studies on pentane that lead to the discovery of Rh_2[*S*-3,5-di(*p*-^{t}BuC_6H_4)TPCP]$_4$, the biphenyl catalyst Rh_2(*S*-*p*-PhTPCP)$_4$ was also evaluated (Figure 3b). Rh_2(*S*-*p*-PhTPCP)$_4$ was expected to be less crowded compared to Rh_2[*S*-3,5-di(*p*-^{t}BuC_6H_4)TPCP]$_4$ and was expected to favor C2 functionalization over C1 functionalization of *n*-alkanes. However, the opposite trend was observed, suggesting that Rh_2(*S*-*p*-PhTPCP)$_4$ was more sterically demanding. The X-ray structure of this catalyst revealed that all of the biphenyl groups occupy the same face. The biaryl rings are involved in π-stacking and this disrupts the C_4 symmetry of a regular α,α,α,α orientation and instead the complex is pseudo C_2 symmetric. Further computational studies will be needed to understand the conformational dynamics of this catalysts in solution but the X-ray structure indicates that the face with the biphenyl groups is more accessible to carbene binding. Also, once the carbene has bound, the birayl ligands would be relatively close to the carbene suggesting that this catalyst would be more sterically demanding Rh_2[*S*-3,5-di(*p*-^{t}BuC_6H_4)TPCP]$_4$.

The profound effect of two meta substituents on the C1 aryl group led us to also explore the behavior of ligands containing groups close to the cyclopropane, such as an *o*-chloro substituent (Figure 3c). The X-ray structure of Rh_2(*S*-*o*-ClTPCP)$_4$ revealed that this complex adopts an α,α,α,α orientation but unlike Rh_2(*p*-PhTPCP)$_4$, the catalyst is C_4 symmetric. In order to accommodate the *o*-chloro-substituent, the aryl rings splay outwards. This causes the *cis*-C2 aryl groups on the other face of the catalyst to be close together (orange rings in Figure 3c), which interferes with ligand coordination to that face. Computational analysis of the energetically lowest conformers of Rh_2(*S*-*o*-ClTPCP)$_4$ (performed at the B3LYP-d3bj level of theory) revealed intimate structural and energetic details consistent with the X-ray data. An α,α,α,α orientation of Rh_2(*S*-*o*-ClTPCP)$_4$, with its C_4 symmetry, was found to be the most stable conformer

with the α,α,α,β conformation 4.3/4.6 kcal/mol higher in energy (presented as ΔH/ΔG). In other words, rotation of one ligand from the α position to the β position is energetically demanding. The α,α,β,β and α,β,α,β conformations are calculated to be even less stable, 5.0/5.2 and 6.6/6.9 kcal/mol higher than the energetically most stable α,α,α,α conformer (see SI for details).

Having discovered that the $Rh_2(TPCP)_4$ catalysts can adopt three distinct orientations we became interested in determining what would be the influence of the structural changes on the site selectivity of C–H functionalization of simple alkanes. C–H functionalization preferentially occurs at electron rich C–H bonds as the C–H insertion is a concerted asynchronous process with build-up of positive charge at carbon. We conducted a study on a range of substrates, with relatively similar steric considerations so that the influence of electronic effects within the substrate on the site-selectivity could be explored. Therefore, a range of terminally-substituted *n*-alkanes were used as substrates and the site-selectivity between C2 and C1 functionalization (and diastereoselectivity) for the three catalysts were determined, using the standard donor/acceptor carbene precursor, trichloroethyl *p*-bromophenyldiazoacetate[8] (Figure 4). The selectivity of the Rh_2[*R*-3,5-di(*p*-^{t}BuC$_6$H$_4$)TPCP]$_4$-catalyzed reactions has been described previously.[8] but a wider range of substrates are reported here. The site selectivity favors C2 but the selectivity decreases progressively from the 1-halohexanes to 1-halobutanes. The C2/C1 site selectivity is 18:1 for 1-bromohexane but is only 3:1 for 1-bromobutane. Similar trends were observed with the chloro and fluoro derivatives, indicating that the inductive effect of the halogen is significant even when the site for C–H functionalization is 3-4 atoms away. Rh_2(*S*-*o*-ClTPCP)$_4$ is even more selective for C2 than Rh_2[*R*-3,5-di(*p*-^{t}BuC$_6$H$_4$)TPCP]$_4$. Except for the reactions with the 1-halobutanes and 1-halopentanes, the reactions with the other substrates give a C2/C1 site selectivity of >25:1 with the best results obtained with trimethylsilylbutane, which gave a site selectivity of 53:1. Therefore, the *o*-chloroaryl scaffold will be worth exploring further to enhance C2 methylene selectivity in complex substrates. However, in the case of the silyl-substituted substrates and *n*-octane, C–H functionalization at other internal methylene sites was also observed. Previously, it was reported that the reaction of pentane with Rh_2(*R*-*p*-PhTPCP)$_4$ has a greater preference for primary C–H functionalization compared to Rh_2[*R*-3,5-di(*p*-^{t}BuC$_6$H$_4$)TPCP]$_4$.[8] This behavior was observed across the entire substrate series. The highest C2/C1 site selectivity with Rh_2(*R*-*p*-PhTPCP)$_4$ was ~4:1, whereas Rh_2[*R*-3,5-di(*p*-^{t}BuC$_6$H$_4$)TPCP]$_4$ yielded up to 34:1 site selectivity with electron rich substrates. In the case of the silyl-substituted substrates, some C–H functionalization at other internal methylene sites was also observed.

Even though this study is emphasizing the influence of the catalysts structure on site selectivity, these chiral catalysts also alter the diastereoselectivity and enantioselectivity of the reactions. The reactions with all three catalysts are moderately diastereoselective with Rh_2(*S*-*o*-ClTPCP)$_4$ generally giving the highest levels of diastereocontrol. As previously reported, the reactions catalyzed by

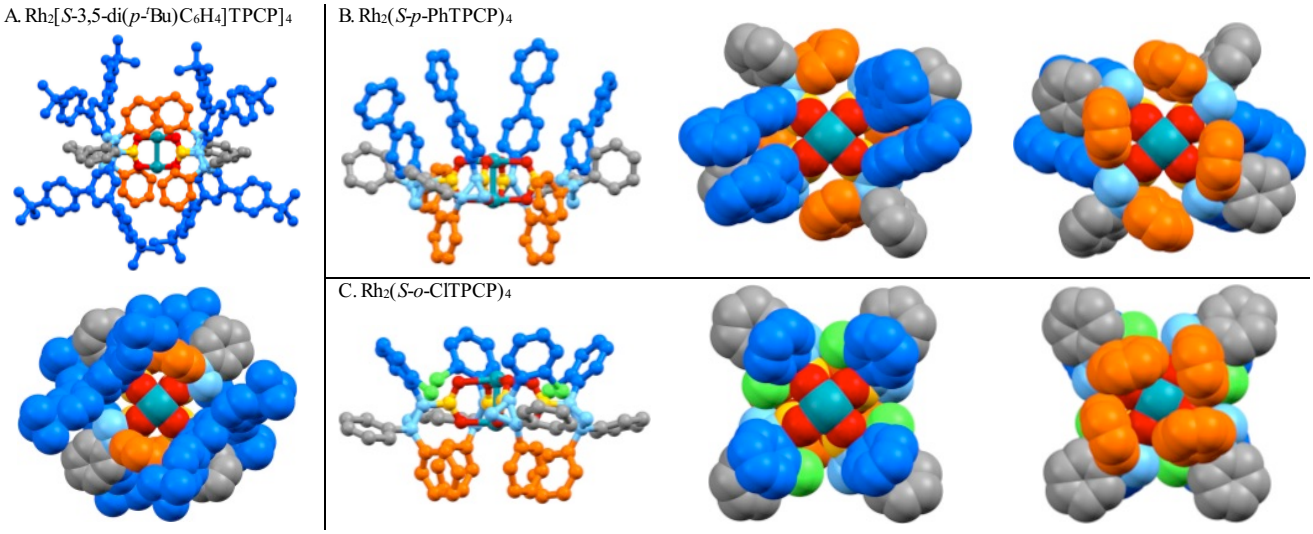

Figure 3. X-Ray structures of Rh_2[*S*-3,5-di(*p*-^{t}Bu)C$_6$H$_4$]TPCP]$_4$, Rh_2(*S*-*p*-PhTPCP)$_4$ and Rh_2(*S*-*o*-ClTPCP)$_4$ (lacking axially coordinated solvent molecules)

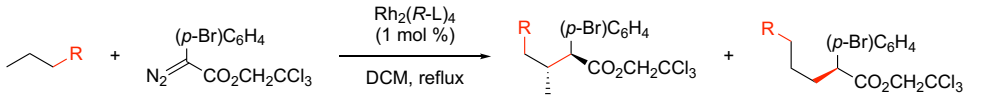

entry	Substrate	Rh_2[*R*-3,5-di(*p*-^{t}BuC$_6$H$_4$)TPCP]$_4$ rr (A:B)	dr (A)	ee (A, %)	yield (A, %)	Rh_2(*R*-*p*-PhTPCP)$_4$ rr (A:B)	dr (A)	yield (A, %)	Rh_2(*S*-*o*-ClTPCP)$_4$ rr (A:B)	dr (A)	ee (A, %)	yield (A, %)
1	Br	18	9	92	89	3	8	81	27	13	82	80
2	Cl	18	9	93	84	3	10	79	30	12	80	78
3	F	18	9	97	85	2	9	79	29	10	83	78
4	Br	9	9	95	65	1	8	77	16	10	81	61
5	Cl	9	9	94	50	2	10	75	17	11	81	56
6	F	8	10	97	49	2	8	78	17	12	84	57
7	Br	3	9	93	20	1	5	71	6	6	79	41
8	Cl	3	7	92	19	1	6	70	6	4	83	40
9	^{t}Bu	33	4	90	89	2	4	82	32	9	76	72
10	TMS	34	4	>99	40	4 [a]	4	80	53 [c]	8	76	72
11	TMS	20	9	90	85	3 [b]	9	86	36 [d]	13	77	66
12		27	9	91	82	2	9	86	30 [e]	12	81	76

The Rh_2[*R*-3,5-di(*p*-^{t}BuC$_6$H$_4$)TPCP]$_4$-catalyzed reactions in entries 1,2,3,4,10-13 have been described previously (Ref 8). A and B were the only C-H functionalization regioisomers observed in the crude ^{1}H NMR spectra unless otherwise noted. Other internal C–H insertion products were observed in the ^{1}H NMR spectra of the crude reaction mixtures of some reactions: *a* 10%; *b* 4%; *c* 7%; *d* 6%; *e* <1% (additional sites of functionalization marked in yellow circles). Enantiomeric excess of Rh_2(*R*-*p*-PhTPCP)$_4$ catalyzed reactions (entry 1-6, 10-12) were not determined due to the low regioisomeric ratio and the corresponding overlap of regioisomer peaks, but enantiomeric excess of the following entries were determined: entry 7: 96% ee, entry 8: 94% ee, entry 9: 88% ee.

Figure 4. Selective C–H functionalization of terminally-substituted *n*-alkanes

Rh_2[*R*-3,5-di(*p*-^{t}BuC$_6$H$_4$)TPCP]$_4$ are highly enantioselective (90->99% ee), whereas the Rh_2(*S*-*o*-ClTPCP)$_4$-catalyzed reactions are less effective (76-84% ee). Overall, the Rh_2(*R*-*p*-PhTPCP)$_4$- catalyzed reactions were the least regio- and diastereoselective. The enantioselectivity of the Rh_2(*R*-*p*-PhTPCP)$_4$-catalyzed reactions were not determined because of poor HPLC resolution caused by the presence of significant amounts of the second regioisomer.

To further investigate the observed site selectivity trends as afunction of substrate, we examined the ability to correlate the outcomes to various physical organic parameters.[11] As a starting point, *para*-substituted benzoic acids (Figure 5A), inspired by Hammett σ-values, were calculated as simulated substrates since the evaluated substrates were intended to only probe electronic variation. The resultant descriptors were assessed in correlations to the regioisomeric ratio energy preferences (reported as a $\Delta\Delta G^{\ddagger}$) using various goodness of fit criteria. Of these, the Natural Bond Orbial (NBO) charge of C4 demonstrated a strong correlation to the observed energy differences for Rh_2[*R*-3,5-di(*p*-^{t}BuC$_6$H$_4$)TPCP]$_4$ (catalyst 1, Figure 5B) and Rh_2(*R*-*p*-PhTPCP)$_4$ (catalyst 2, Figure 5C). NBO charges of carbonyls adjacent to benzene rings have been correlated to Hammett σ-values previously so this outcome is consistent with the NBO charge reading out[12] the relative electronic perturbations of the substrates. While this is somewhat intuitive, the sensitivity of the NBO calculation provides a platform for the rapid assessment of electronics and prediction of similar simple substrates. Additionally, as the same parameter is able to describe two catalysts, it was hypothesized that this charge would also correlate to the outcomes from Rh_2(*S*-*o*-ClTPCP)$_4$ (catalyst 3, Figure 5D) and we anticipated that the relative slope of only a few substrates could be used to predict all other substrates relatively well. Therefore, the empirical results using 1-bromohexane and 1-chloropentane as substrates with catalyst 3 were applied to define the slope and intercept of a prediction equation. Examining the

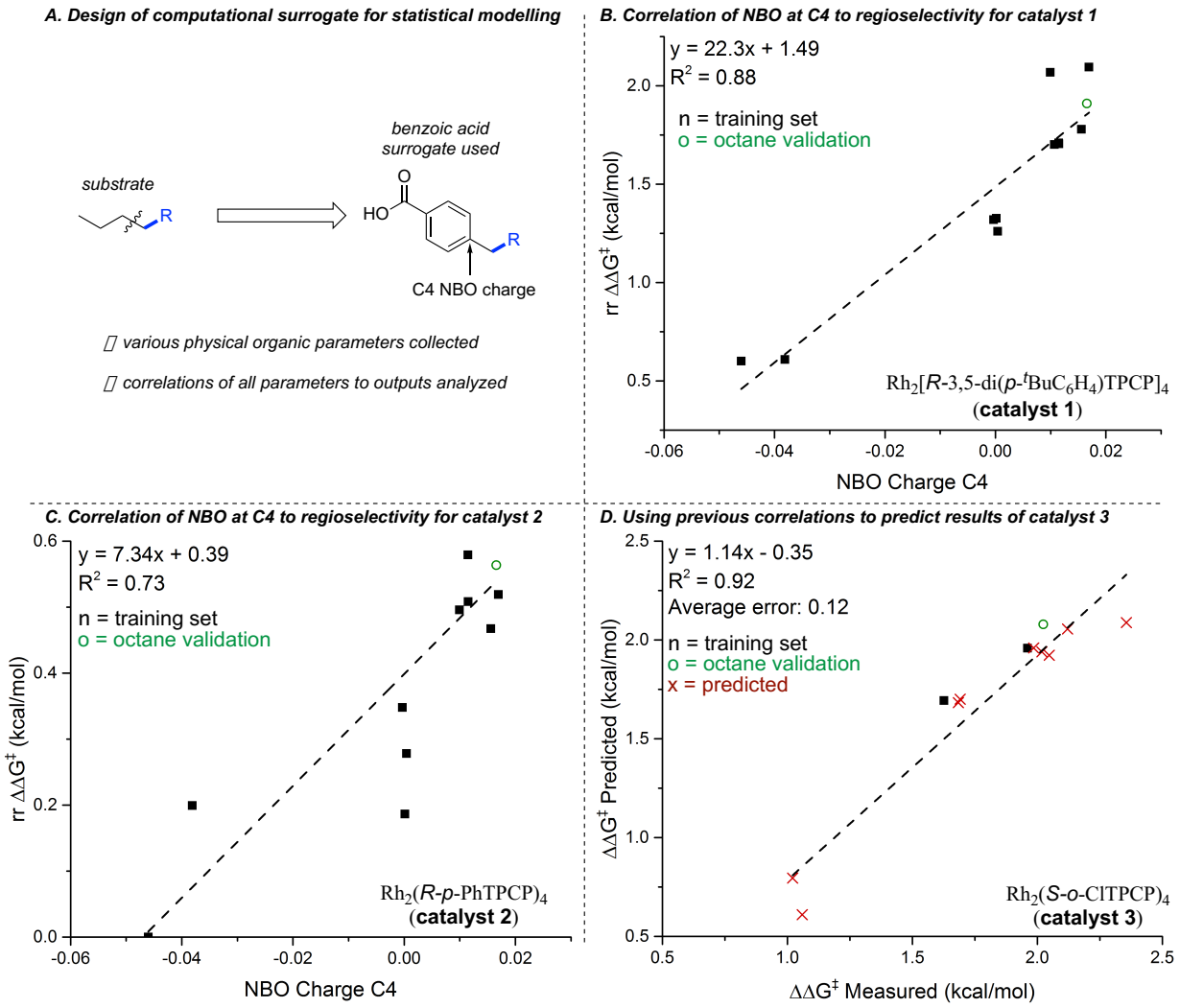

Figure 5. Simultated charges on a benzoic acid derived substrate surrogates described regioselectivity for all three catalysts.

other data points, an excellent agreement is observed between measured and predicted regioisomeric ratio. This provides confidence when new catalysts are evaluated that only a few data points should be required to predict the outcomes of a wide range of functionalized n-alkanes. Additionally, these data suggest that this catalyst class functions in a similar manner across different symmetry orientations providing the foundation for future mechanistic interrogation.

In conclusion, these studies reveal that the $Rh_2(TPCP)_4$ catalysts can adopt at least three high symmetry orientations, which is dependent on the frame work of the cyclopropane. Rh_2[*S*-3,5-di(*p*-^{t}BuC_6H_4)TPCP]$_4$ preferentially adopts a D_2 symmetric arrangement, whereas the X-ray structure of Rh_2(*S*-*o*-ClTPCP)$_4$ adopts a C_4 symmetric structure and Rh_2(*S*-*p*-PhTPCP)$_4$ is pseudo C_2 symmetric. Rh_2[*S*-3,5-di(*p*-^{t}BuC_6H_4)TPCP]$_4$ and Rh_2(*S*-*o*-ClTPCP)$_4$ are both selective for C–H functionalization at the most accessible secondary site. Rh_2(*S*-*p*-PhTPCP)$_4$ is not particularly selective but it does represent the catalyst that gives the most preference towards the primary C–H reported thus far. Even though the catalysts have different ligand arrangements and selectivity profiles, it is still possible to develop a quantitative model for these catalysts that allows a useful correlation for their behavior without need to evaluate a significant number of substrates. Future work will integrate the information gained in this study into more extensive computational studies and to the design of even more site-selective catalysts.

ASSOCIATED CONTENT

AUTHOR INFORMATION

Corresponding Authors

hmdavie@emory.edu
dmusaev@emory.edu
matt.sigman@utah.edu.

Notes

HMLD is a named inventor on a patent entitled, Dirhodium Catalyst Compositions and Synthetic Processes Related Thereto (US 8,974,428, issued 3/10/2015). The other authors have no competing financial interests.

Supporting Information

Synthetic details and spectral data. This material is available free of charge via the Internet at http://pubs.acs.org.

ACKNOWLEDGMENT

Financial support was provided by NSF under the CCI Center for Selective C–H Functionalization (CHE-1700982). MSS acknowledges the use of the resources of the Center for High Performance Computing at the University of Utah. D.G.M. acknowledges NSF MRI-R2 grant (CHE-0958205) and the use of the resources of the Cherry Emerson Center for Scientific Computation. Funds to purchase the NMR and X-ray spectrometers used in these studies were supported by NSF (CHE 1531620 and CHE 1626172). We thank Dan Morton for assistance in preparing the visual in Figure 2.

REFERENCES

(1) Selected reviews: (a) Crabtree, R. H.; Lei, A. *Chem. Rev.* **2017**, 117, 8481–8482. (b) Yamaguchi, J.; Yamaguchi, A. D.; Itami, K. *Angew. Chem. Int. Ed.* **2012**, 51, 8960–9009. (c) Gutekunst, W. R.; Baran, P. S. *Chem. Soc. Rev.* **2011**, 40, 1976–1991.

(2) (a) Romero, N. A.; Margrey, K. A.; Tay, N. E.; Nicewicz, D. A. *Science* **2015**, 349, 1326–1330. (b) Cuthbertson, J. D.; MacMillan, D. W. *Nature* **2015**, 519, 74–77. (c) Jin, J.; MacMillan, D. W, *Nature* **2015**, 525, 87–90.

(3) (a) Lyons, T. W.; Sanford, M. S. *Chem. Rev.* **2010**, 110, 1147–1169. (b) Simmons, E. M.; Hartwig, J. F. *Nature* **2012**, 483, 70–73. (c) Zhang, Z.; Tanaka, K.; Yu, J.-Q. *Nature* **2017**, 543, 538-542, and cited references..

(4) Selected articles: (a) Cook, A. K.; Schimler, S. D.; Matzger, A. J.; Sanford. M. S. *Science* **2016**, 351, 1421-1424. (b) Hartwig, J. F.; Larsen, M. A. *ACS Cent. Sci.* **2016**, **2**, 281–292.

(5) (a) Bess, E. N.; Guptill, D. M.; Davies, H. M. L. Sigman, M. S. *Chem. Sci.* **2015**, 6, 3057-3062. (b) Bess, E. N.; DeLuca, R. J.; Tindall, D. J.; Oderinde, M. S.; Roizen, J. L.; Bois, J. D.; Sigman, M. S. *J. Am. Chem. Soc.* **2014**, 136, 5783–5789. (c) Gormisky, P. E.; White, M. C. *J. Am. Chem. Soc.* **2013**, 135, 14052–14055.

(6) (a) Davies, H. M. L.: Hansen, T.; Churchill, M. R. *J. Am. Chem. Soc*. **2000**, 122, 3063–3070. (b) Davies, H. M. L.; Morton, D. *Chem. Soc. Rev*. **2011**, 40, 1857-1869.

(7) (a) Qin, C.; Boyarskikh, V.; Hansen, J. H.; Hardcastle, K. I.; Musaev, D. G.; Davies, H. M. L. *J. Am. Chem. Soc.* **2011**, 133, 19198–19204. (b) Qin, C. M.; Davies, H. M. L. *J. Am. Chem. Soc.* **2014**, 136**,** 9792–9796. (c) Guptill, D. M.; Davies, H. M. L. *J. Am. Chem. Soc.* **2014**, 136, 17718–17721.

(8) Liao, K.; Negretti, S.; Musaev, D. G.; Bacsa, J.; Davies, H. M. L. *Nature* **2016**, 533, 230–234.

(9) (a) Davies, H. M. L.; Bruzinski, P. R.; Lake, D. H.; Kong, N.; Fall, M. J. *J. Am. Chem. Soc.* **1996**, 118, 6897–6907. (b) Hansen, J.; Thompson, J.; Davies, H. M. L. *Coord. Chem. Rev.* **2008**, 252, 545-555.

(10) (a) Lindsay, V. N. G.; Lin, W.; Charette, A. B. *J. Am. Chem. Soc.* **2009**, 131, 16383–16385. (b) DeAngelis, A.; Dmitrenko, O.; Yap, G. P. A.; Fox, J. M. *J. Am. Chem. Soc.* **2009**, 131, 7230–7231.

(11) Sigman, M. S.; Harper, K. C.; Bess, E. N.; Milo, A. *Acc. Chem. Res.* **2016,** 49, 1292-1301.

(12) (a) Reed, A. E.; Weinstock, R. B.; Weinhold, F. *J. Chem. Phys.* **1985,** 83, 735-746. (b) Glendening, E. D.; Landis, C. R.; Weinhold, F. *J. Comput. Chem.* **2013,** 34, 1429-1437. (c) Santiago, C. B.; Milo, A.; Sigman, M. S. *J. Am. Chem. Soc.* **2016,** 138, 13424-13430.

TOC Graphic

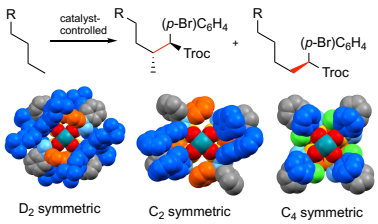
R
catalyst-
controlled
R
(p-Br)C6H4
Troc
+
R
(p-Br)C6H4
Troc
D2 symmetric
C2 symmetric
C4 symmetric